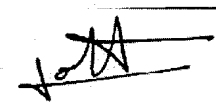
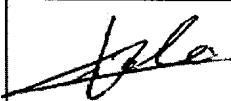

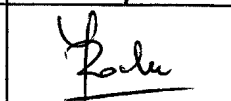
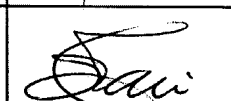
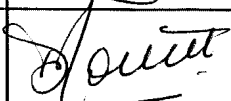
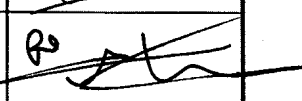


HERSCHEL / PLANCK

**HERSCHEL Micro-Vibration Analysis Report
H-P-2-ASP-AN-0773**

	Function Name	Date	Signature
Rédigé par/ <i>Written by</i>	Mechanical Analyses Team	01/08/06	
Vérifié par/ <i>Verified by</i>	Sciences/Obs. Satellite Group Manager R. VIALE	08/08/06	
Approbation/ <i>Approved by</i>	System Mechanical Architecture Ph. CLAVEL	28/09/06	
Approbation/ <i>Approved by</i>	Herschel Technical Responsible Y. ROCHE	29/09/06	
Approbation/ <i>Approved by</i>	PA Manager T. GRASSIN	07/10/06	
Approbation/ <i>Approved by</i>	Herschel Satellite Manager D. MONTET	29/09/06	
Approbation/ <i>Approved by</i>	Project Manager J.J. JUILLET	3.10.06	

Entité Emettrice : Alcatel Space - Cannes
(détentrice de l'original) :

HERSCHEL/PLANCK		DISTRIBUTION RECORD	
DOCUMENT NUMBER : H-P-2-ASP-AN-0773		Issue 2/ Rev. : 0 Date: 31/07/2006	
EXTERNAL DISTRIBUTION		INTERNAL DISTRIBUTION	
ESA	X	HP team	X
ASTRIUM			
ALENIA			
CONTRAVES			
TICRA			
TECNOLOGICA			
		Clf Documentation	Orig.

ENREGISTREMENT DES EVOLUTIONS / CHANGE RECORDS

ISSUE	DATE	§ : DESCRIPTION DES EVOLUTIONS § : CHANGE RECORD	REDACTEUR AUTHOR
2	31/07/2006	Signature table changed Paragraph §6.2 deleted Conclusions updated RD 6 added	D. JOLLET

TABLE OF CONTENTS

1	APPLICABLE & REFERENCE DOCUMENTS	8
2	INTRODUCTION	9
3	HERSCHEL SPACECRAFT	10
3.1	MCI	11
4	REACTION WHEELS	12
5	MICRO-VIBRATION ANALYSIS	14
5.1	NASTRAN analysis	15
5.2	MICROVISION analysis	16
6	RESULTS	17
6.1	Contribution of each Reaction Wheel separately	18
6.2	Sensitivity on the damping factor	19
6.3	Results for the four wheels simultaneously	20
7	CONCLUSIONS	22
7.1	Analysis Conclusions	22
7.2	Test Results	22
7.3	New Reaction Wheel Profiles	22
	APPENDIX 1 : EXCITATION FORCE INPUT	23

LIST OF TABLES

TABLE 1	12
TABLE 2	16

LIST OF FIGURES

FIGURE 1:HERSCHEL SPACECRAFT FEM VIEW	10
FIGURE 2 : MODEL OF REACTION WHEELS MOUNTED ON Z+/Y- PANEL	13
FIGURE 3 : RESPONSE AT NODE 48301 DUE TO REACTION WHEEL 1 (NODE 17188)	18
FIGURE 4 : RESPONSE AT NODE 48301 DUE REACTION WHEEL 2 (NODE 17189)	18
FIGURE 5 : RESPONSE AT NODE 48301 DUE TO REACTION WHEEL 3 (NODE 17186)	18
FIGURE 6 : RESPONSE AT NODE 48301 DUE TO REACTION WHEEL 4 (NODE 17187)	18
FIGURE 7 : SPEED PROFILE WHEEL 1 (NODE 17188)	20
FIGURE 8 : SPEED PROFILE WHEEL 2 (NODE 17189)	20
FIGURE 9 : SPEED PROFILE WHEEL 3 (NODE 17186)	20
FIGURE 10 : SPEED PROFILE WHEEL 4 (NODE 17187)	20
FIGURE 11	21
FIGURE 12 : RADIAL EXCITATION FORCE GIVEN BY TELDIX	23
FIGURE 13 : RADIAL EXCITATION FORCE INPUT	23
FIGURE 14 : AXIAL EXCITATION FORCE GIVEN BY TELDIX	24
FIGURE 15 : AXIAL EXCITATION FORCE INPUT	24

1 APPLICABLE & REFERENCE DOCUMENTS

- [RD1] ACMS Glossary_update
H-P-4-DS-TN-017_2_0
- [RD2] CDR Herschel Dynamic Analysis and Sine Test Prediction Report
H-P-2-ASPI-AN-0719, Issue 1.0
- [RD3] Duch Space /SENER ACMS
H-P-4 ANA-TN-006, Issue 3.0
- [RD4] RFD Duch space
HP-TX-RFD-0003 rev 1 dated 02/12/03
- [RD5] Herschel /Planck Instrument Interface Document part B instrument "SPIRE"
SCI-PT-IIDB/SPIRE-02124 Issue 3.2 dated 01/03/04
- [RD6] HERSCHEL STM Micro-vibrations Test Report
H-P-2-ASP-TR-1110

Software version:

- Nastran 70.
- Microvision 4.2.
- Matlab6.5.

2 INTRODUCTION

Micro vibrations are critical for the SPIRE instrument of the Herschel spacecraft. They generate disturbing vibrations on the focal plane equipment.

The main source of perturbation identified is the four reaction wheels used to adjust the orientation of Herschel. They are operating at a rotating speed which may vary between 0 and 45 Hz. The AOCS profile taken into account is given in ref. [3]. The wheels are characterised by their static imbalance that generate a radial force and by an axial force. They are both applied at the centre of Gravity of the wheel. Considering the results from PDR phase and checked by primary CDR analysis, the dynamic imbalance that represents less than 2% of the perturbation has not been taken into account.

The aim of this analysis is to determine the level of acceleration at the centre of gravity of the SPIRE FPU due to the reaction wheels perturbation.

3 HERSCHEL SPACECRAFT

HERSCHEL spacecraft f.e.m. view:

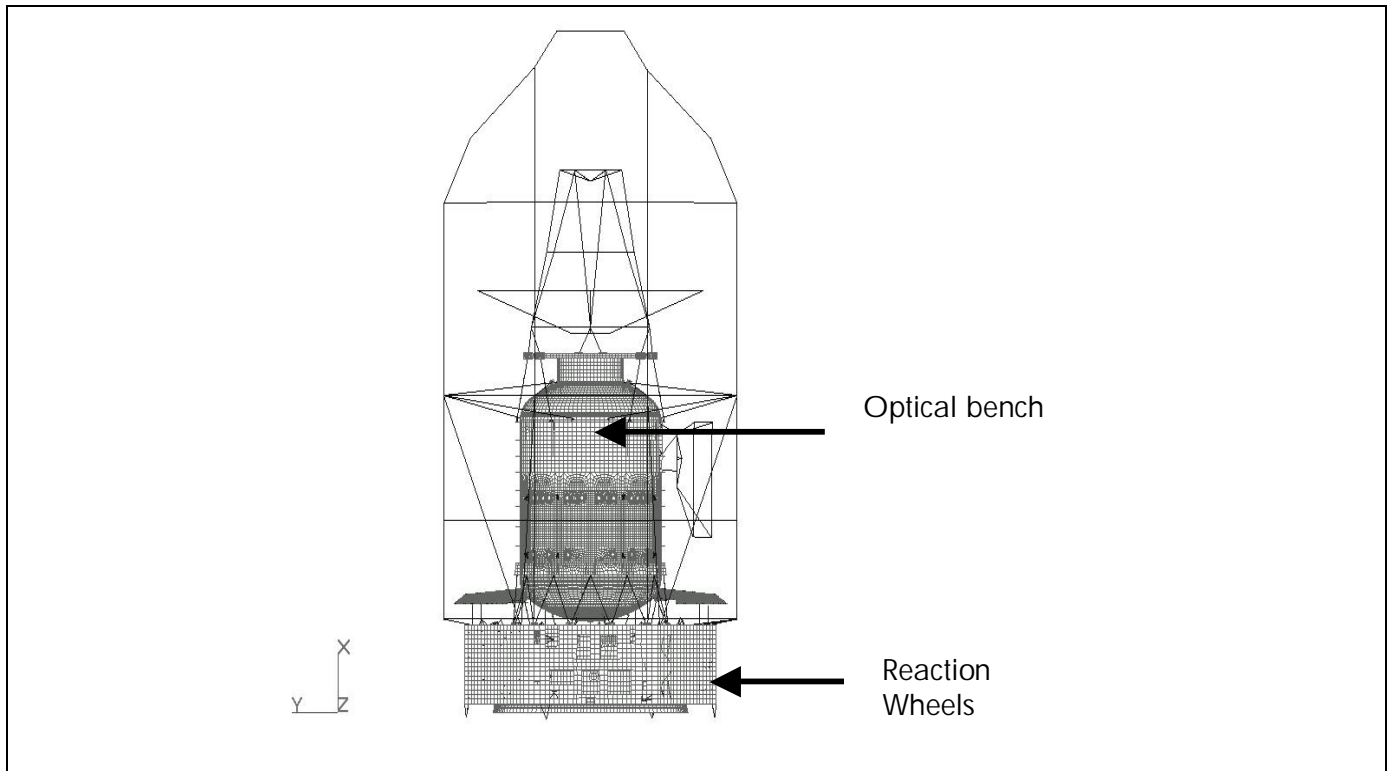


Figure 1:HERSCHEL spacecraft fem view

The structural damping factor has been set to 0.5% to consider a structural damping adapted to microvibration.

The model used for this analysis is described in [RD2].

3.1 MCI

The following table shows spacecraft cog and mass properties.

O U T P U T F R O M G R I D P O I N T W E I G H T G E N E R A T O R						
REFERENCE POINT = 0						
M O						
*	3.382553E+03	-3.583693E-10	-1.802785E-09	1.635470E-09	-1.946209E+00	-4.064157E+00 *
*	-3.583693E-10	3.382553E+03	3.695160E-10	1.949139E+00	-1.277222E-09	6.733414E+03 *
*	-1.802785E-09	3.695160E-10	3.382553E+03	4.006843E+00	-6.733414E+03	-4.656568E-10 *
*	1.635470E-09	1.949139E+00	4.006843E+00	4.468877E+03	1.861800E+02	-5.847768E+02 *
*	-1.946209E+00	-1.277222E-09	-6.733414E+03	1.861800E+02	2.160342E+04	1.404142E+00 *
*	-4.064157E+00	6.733414E+03	-4.656568E-10	-5.847768E+02	1.404142E+00	2.207971E+04 *
S						
*	1.000000E+00	0.000000E+00	0.000000E+00	*		*
*	0.000000E+00	1.000000E+00	0.000000E+00	*		*
*	0.000000E+00	0.000000E+00	1.000000E+00	*		*
DIRECTION						
MASS AXIS SYSTEM (S)	MASS	X-C.G.	Y-C.G.	Z-C.G.		
X	3.382553E+03	4.835017E-13	1.201506E-03	-5.753667E-04		
Y	3.382553E+03	1.990630E+00	-3.775910E-13	-5.762331E-04		
Z	3.382553E+03	1.990630E+00	1.184562E-03	-1.376643E-13		
I (S)						
*	4.468872E+03	-1.941561E+02	5.886569E+02	*		*
*	-1.941561E+02	8.199684E+03	-1.401804E+00	*		*
*	5.886569E+02	-1.401804E+00	8.675973E+03	*		*
I (Q)						
*	8.208247E+03			*		*
*		4.378357E+03		*		*
*			8.757924E+03	*		*
Q						
*	-4.361448E-02	-9.894923E-01	1.378507E-01	*		*
*	-9.976985E-01	5.030945E-02	4.546009E-02	*		*
*	-5.191760E-02	-1.355507E-01	-9.894092E-01	*		*

The spacecraft total mass is 3382 kg. A complete description of the HERSCHEL fem is given in [RD2].

4 REACTION WHEELS

Each reaction wheel is represented by a rigid body connecting together its 4 interface points enabling introduction of interface disturbances (Figure 2).

Wheel number	Node ID	Analysis Coordinate System
1	17188	13003
2	17189	13002
3	17186	13004
4	17187	13001

Table 1

The disturbance is modelled as a radial force and an axial force that are both applied at the centre of Gravity of the wheel (ref. annex 1)

A local rectangular co-ordinate system is attached to each wheel and defined as follows:

- Origin at the centre of gravity of the wheel
- Y direction parallel to the wheel rotation axis
- (X, Z) plane parallel to the wheel mounting plane

The SPIRE optical instrument is represented by a point mass connected to the structure with a rigid body element. It is assumed that there is no mode local to the optical instrument below 350Hz. Outputs of the computations are presented at its CoG. The node corresponding to the optical instrument is node 48301.

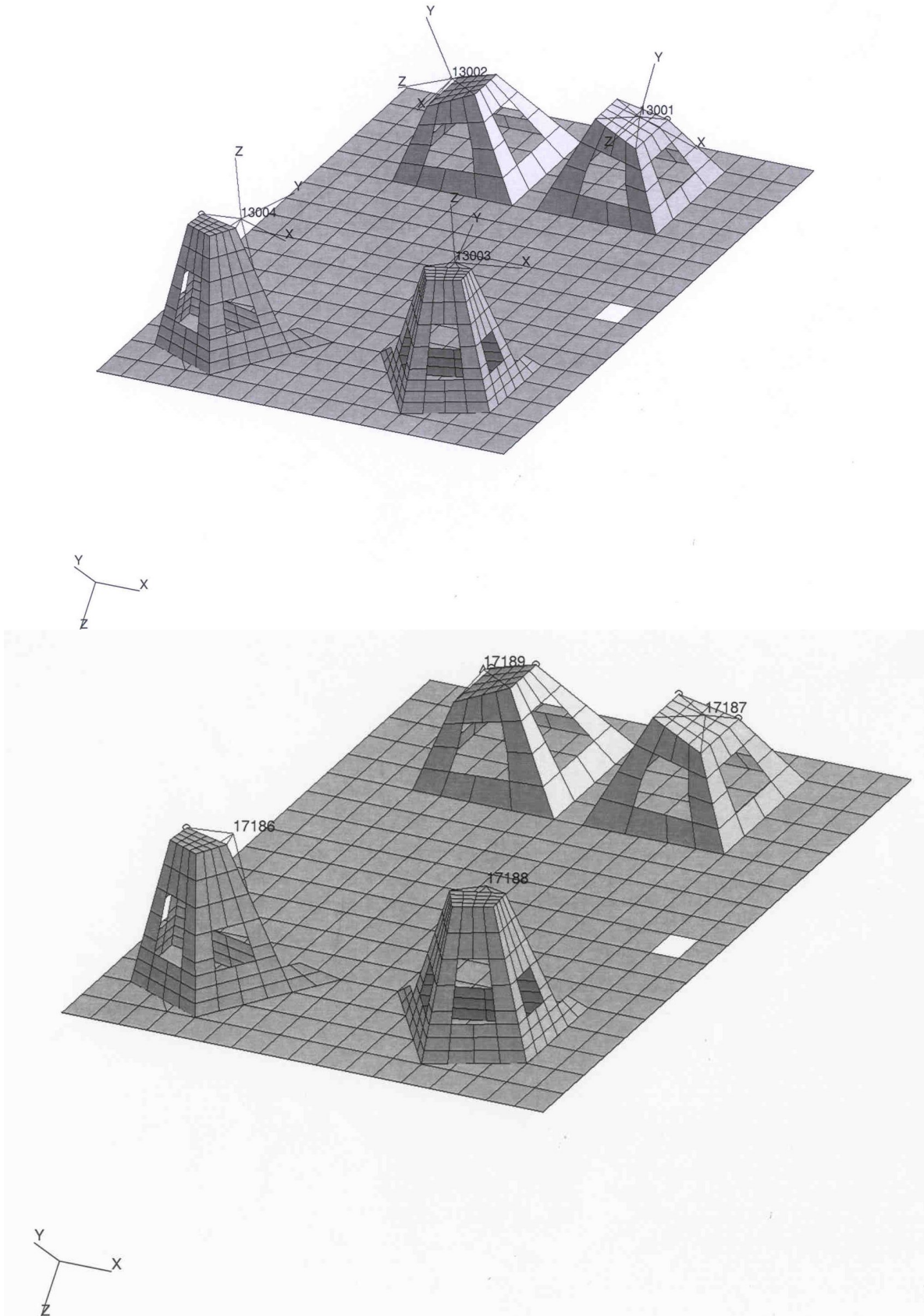


Figure 2 : Model of reaction wheels mounted on Z+/Y- panel

5 MICRO-VIBRATION ANALYSIS

5.1 NASTRAN analysis

The Nastran model used is the same as the one from sine analysis described in ref. [2]. Therefore the model is representative of the Herschel dynamic behaviour up to 140 Hz. Results at higher frequencies must be considered with caution. Nevertheless the main contribution to the Spire optical instrument, which dynamical behaviour is taken into account in the model with as spring-mass system, occurs below 120 Hz (see figure 7; maximum responses due to $16.4 \cdot 6 \approx 98.3$ Hz; $19.6 \cdot 5 \approx 98.3$ Hz; $24.56 \cdot 4 = 98.3$ Hz; $32.8 \cdot 3 \approx 98.3$ Hz)

The only differences between the sine model and the one used here are the damping factor (0.005), the boundary conditions that are now free-free. The modal analysis is performed between 0 and 300Hz and the modes are normalised to the generalised mass of the Herschel S/C.

The output of the analysis includes the modal displacement, for each mode, at the SPIRE FPU as well as at the nodes representing the reaction wheels.

5.2 MICROVISION analysis

The data required to perform the microvibration analysis are the following:

- A Nastran punch file containing the modes (up to 300Hz) as well as modal displacements at the reaction wheels and at the Spire instrument location.
- Modal damping is set to 0.005.
- Characteristics of the wheels:
 - Rotating speed of the wheel: 0 to 45Hz.
 - Static Imbalance: 2×10^{-5} kg.m for the first harmonic (guaranteed by TELDIX) The relative contribution of the harmonics is extracted from the ref. [4]. Nine harmonics are taken into account for each excitation-axis. The harmonic 0.59 has been taken into account, it is typical of bearing cage excitation. According to previous studies, its amplitude is set to 2.487×10^{-6} kg.m.

Harmonic number	Radial excitation	Axial excitation
	Static imbalance (kg,m)	Static imbalance (kg,m)
0,59	2,487E-06	2,487E-06
1	2,000E-05	2,000E-05
2	3,420E-07	4,559E-07
3	3,206E-07	4,328E-07
4	3,180E-07	4,266E-07
5	3,161E-07	4,187E-07
6	3,103E-07	4,116E-07
7	3,078E-07	4,104E-07
8	3,040E-07	4,053E-07
9	2,337E-07	2,922E-07

Table 2

Excitation force input: see appendix 1

- The axial excitation are not totally negligible (see measured curve annex A). In conservative way, the radial static imbalance is considered for the 0.59 and 1 harmonic.
- The first analysis is conducted wheel by wheel, for frequencies from 0 to 300 Hz and for wheel velocity varying from 0 to 45Hz. Results provided below are the quadratic sum of the contribution of all harmonics whose frequency is below 300Hz.
- The second analysis is conducted with the four wheels rotating at the same time following the profile given in ref. [3]. Result provided below is a time-acceleration representing the accelerations of the SPIRE CoG during a 5000 seconds phase.
- Outputs are provided at node 48301, CoG of the SPIRE instrument. No specification was provided, therefore results are given in the spacecraft coordinate system.

6 RESULTS

All results are expressed in the Spacecraft coordinate system.

6.1 Contribution of each Reaction Wheel separately

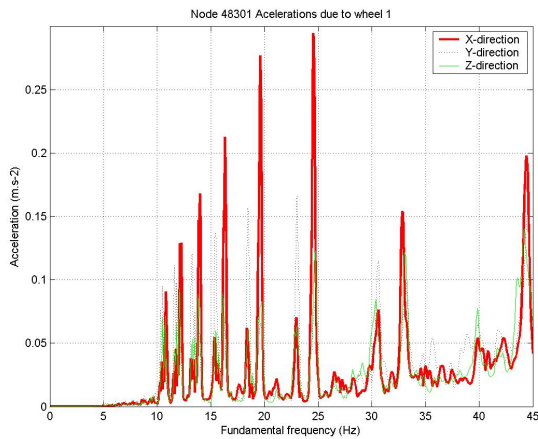


Figure 3 : RESPONSE AT NODE 48301 DUE TO REACTION WHEEL 1 (node 17188)

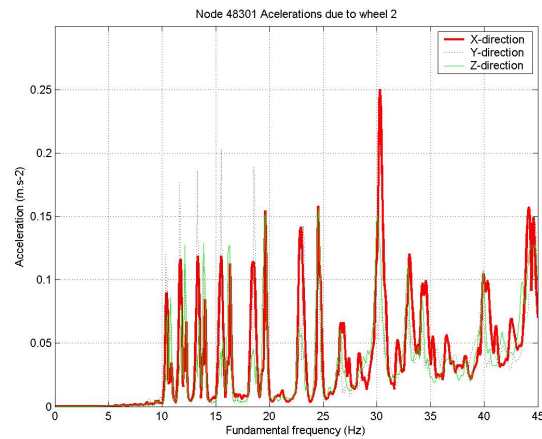


Figure 4 : RESPONSE AT NODE 48301 DUE TO REACTION WHEEL 2 (node 17189)

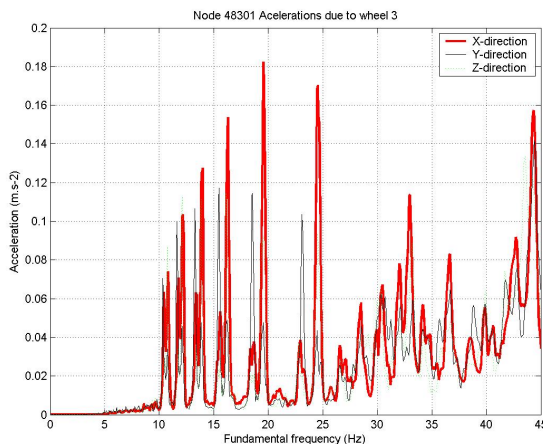


Figure 5 : RESPONSE AT NODE 48301 DUE TO REACTION WHEEL 3 (node 17186)

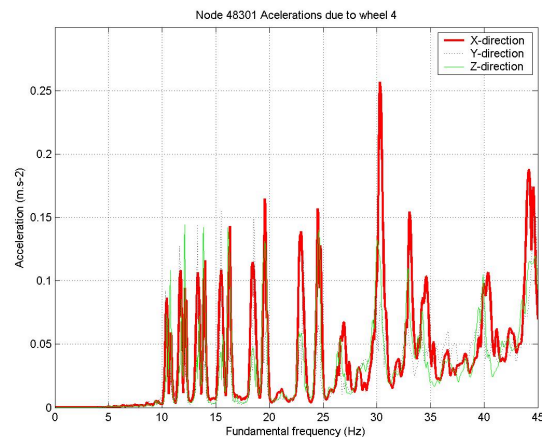


Figure 6 : RESPONSE AT NODE 48301 DUE TO REACTION WHEEL 4 (node 17187)

In this section the contribution of each wheel to the response at the SPIRE optical instrument is computed and presented in Figures 3 to 6.

The maximum acceleration is as follows:

- Due to Reaction Wheel 1: Maximum acceleration occurs at 24.6 Hz with an amplitude of 29 mg in the X direction (see Figure 3).
- Due to Reaction Wheel 2: Maximum acceleration occurs at 30.3 Hz with an amplitude of 25 mg in the X direction (see Figure 4).
- Due to Reaction Wheel 3: Maximum acceleration occurs at 24.6 Hz with an amplitude of 18.3 mg in the X direction (see Figure 5).
- Due to Reaction Wheel 4: Maximum acceleration occurs at 30.3 Hz with an amplitude of 26 mg in the X direction (see Figure 6).

With the previous issue of the document Wheel profile, the SPIRE acceleration are similar (15 mg). The difference is due to the new wheel profile (see appendix 1, with the wheel dynamic behaviour).

6.2 Sensitivity on the damping factor

Chapter deleted as the damping factor found during tests is coherent with the damping factor used in these analyses.

6.3 Results for the four wheels simultaneously

As no statistical analysis has been conducted between each wheel, they are considered in phase. In this case, each wheel speed corresponds to the profile given below (cf. ref. [3]) :

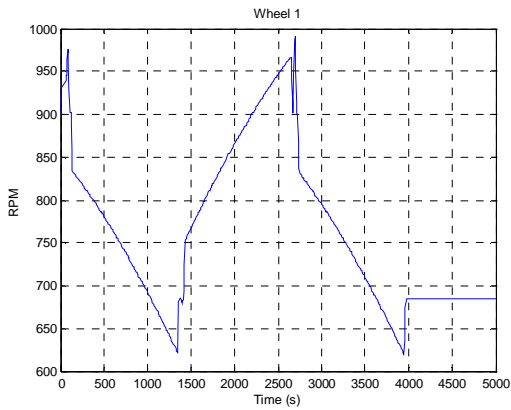


Figure 7 : SPEED PROFILE WHEEL 1 (node 17188)

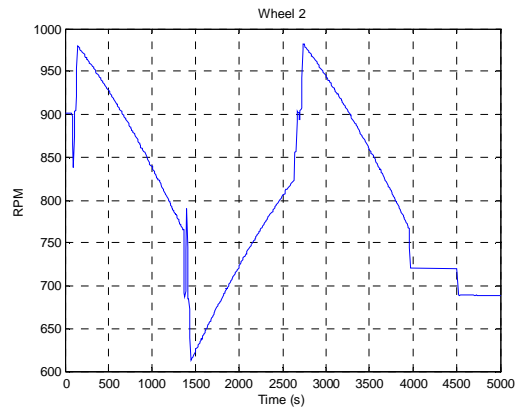


Figure 8 : SPEED PROFILE WHEEL 2 (node 17189)

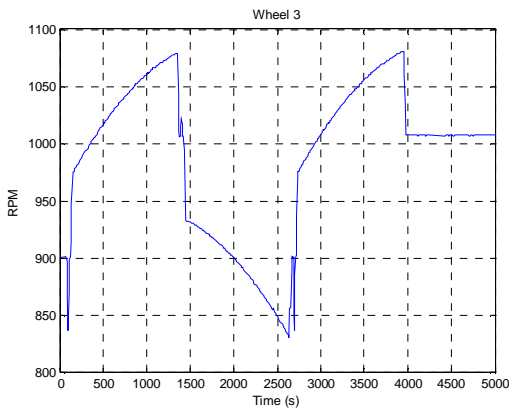


Figure 9 : SPEED PROFILE WHEEL 3 (node 17186)

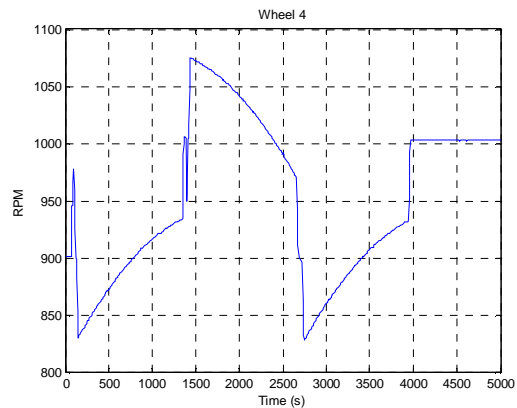


Figure 10 : SPEED PROFILE WHEEL 4 (node 17187)

Result:

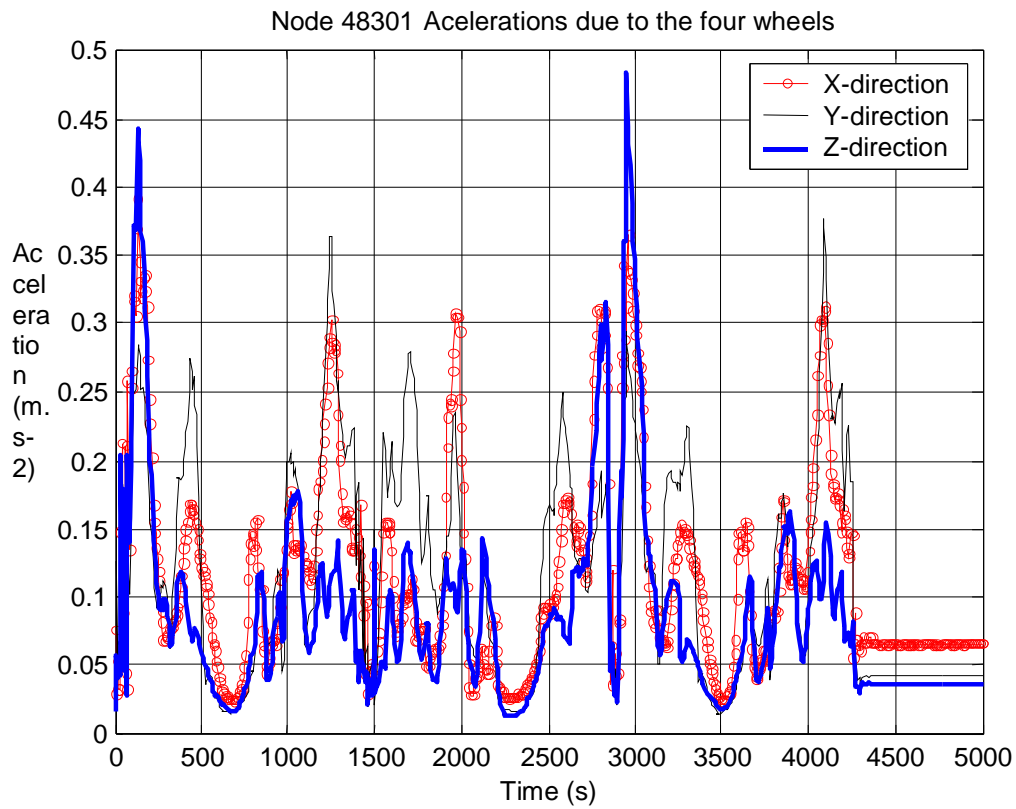


Figure 11

The maximal acceleration occurs after 125 s and has an amplitude of 39 mg in X-axis direction.
 The maximal acceleration occurs after 4087 s and has an amplitude of 37 mg in Y-axis direction.
 The maximal acceleration occurs after 2950 s and has an amplitude of 48 mg in Z-axis direction.

7 CONCLUSIONS

7.1 Analysis Conclusions

The maximum acceleration obtained with one reaction wheel is 29 mg (wheel 1 excitation) at a rotating speed of 24.6 Hz in Spacecraft direction. This acceleration is mainly due to the radial wheel excitation. Wheels 2 and 4 give almost the same level.

Acceleration levels obtained with the four wheels together following the given profile leads to a maximal acceleration level of 48 mg in Z-axis direction after 2900s.

7.2 Test Results

Micro-vibration tests were performed on the spacecraft Herschel STM. In the STM configuration, the reaction wheels were not mounted on, so the excitation was directly induced on their mounting panel by a mini-shaker.

The micro-vibration test results (see [RD6]) were in line with the predictions performed on the STM micro-vibration test configuration.

It can be inferred that both the methodology of analysis and finite element model are correct.

7.3 New Reaction Wheel Profiles

The flight model (FM) reaction wheels have been tested and their input levels are at some frequency range two times higher than the estimated profiles provided by TELDIX and used for the present analysis (New levels are given in H-P-370000-DS-RD-004 iss2).

Thus, the maximum acceleration level achieved with the 4 wheels working is twice that computed in the present analysis, that is to say 96 mg.

APPENDIX 1 : EXCITATION FORCE INPUT

Radial excitation: (249 Hz:12.9 N; 241 Hz:5.7N; 264 Hz:4.4N; 234 Hz:3.2 N; 107Hz:1N; 83Hz:0.2 N; 33 Hz:0.23 N)

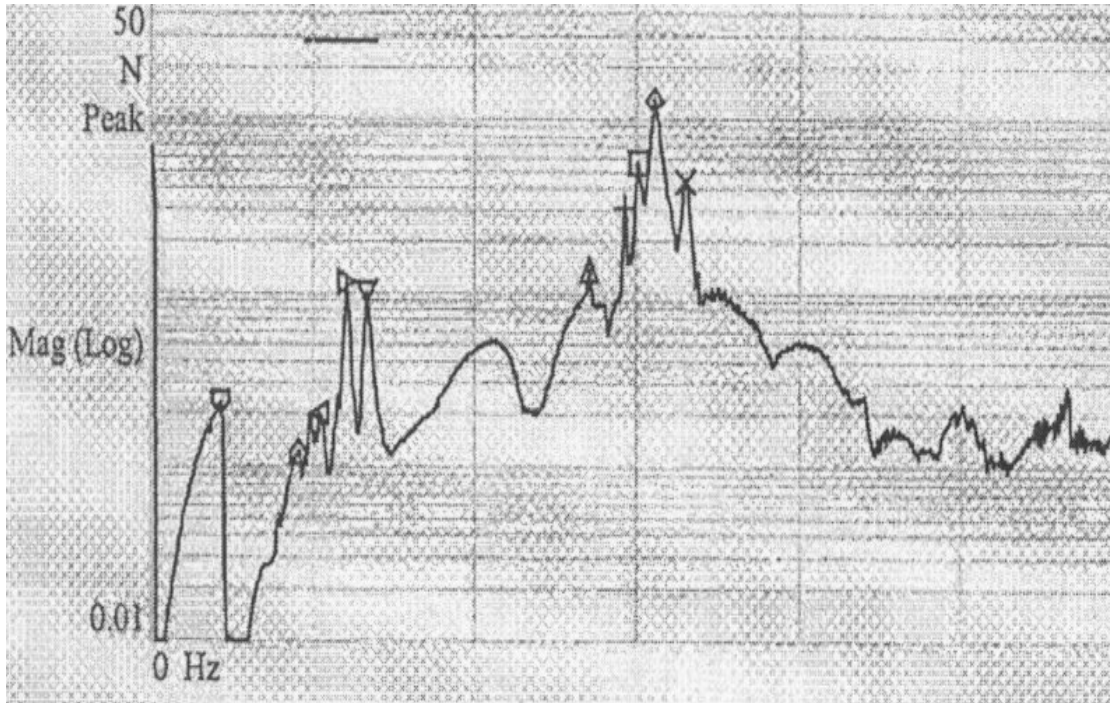


Figure 12 : Radial excitation force given by TELDIX

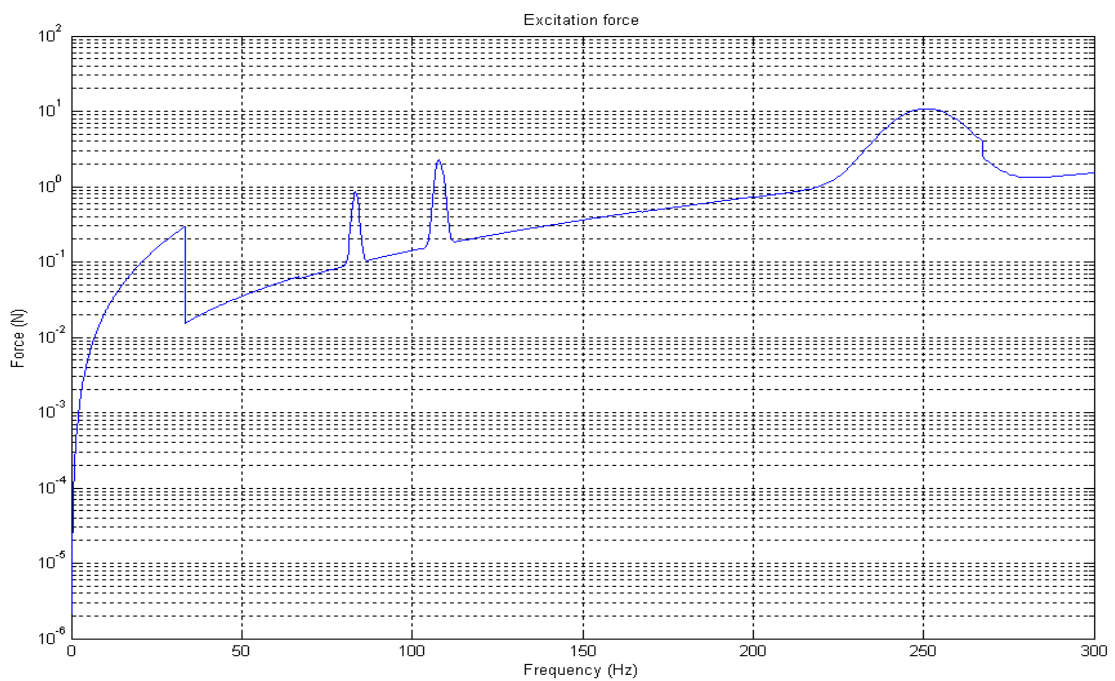


Figure 13 : Radial excitation force input

Axial excitation: (240 Hz:56 N; 234 Hz:18 N; 50Hz:0.056N)

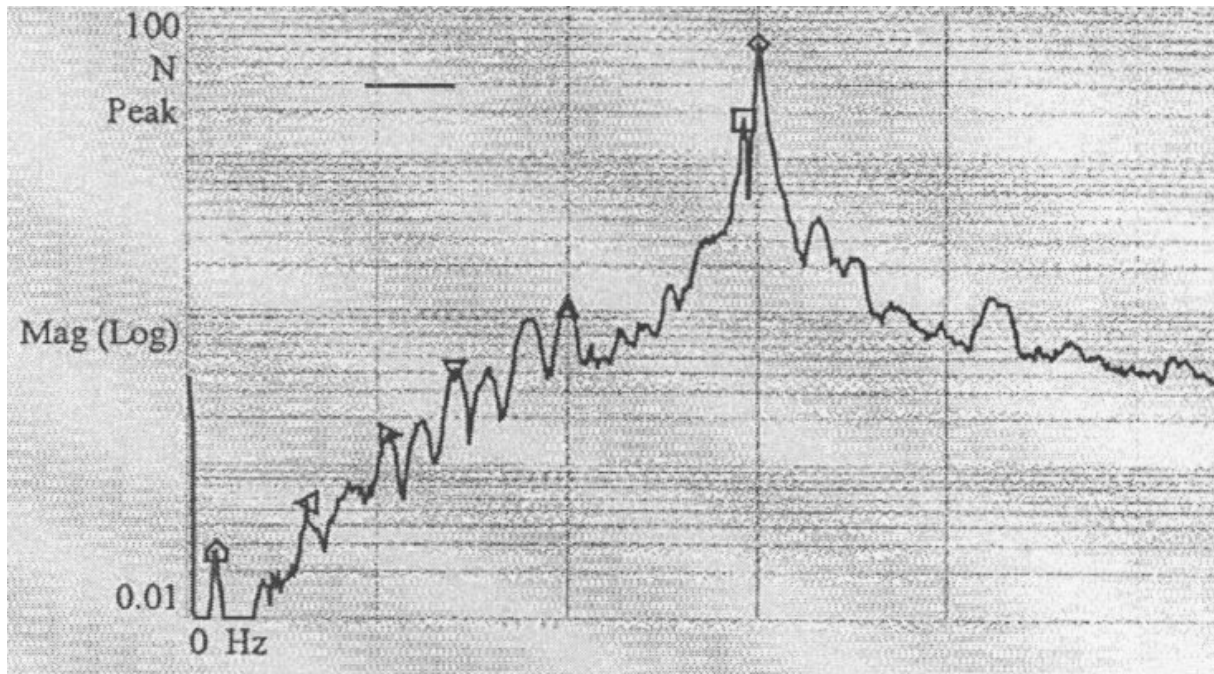


Figure 14 : Axial excitation force given by TELDIX

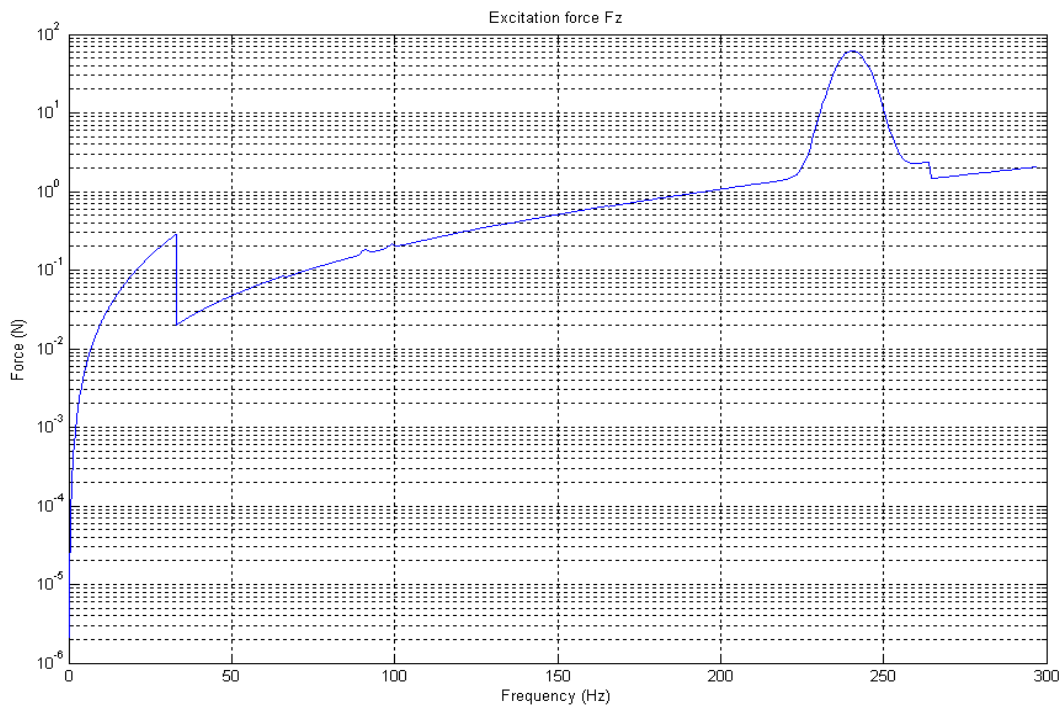


Figure 15 : Axial excitation force input

END OF DOCUMENT